Simulation of the stress dependence of hysteresis loss using an energy-based domain model

AUTHOR(S):

Shumpei, Ito; Takeshi, Mifune; Tetsuji, Matsuo; Chikara, Kaido; Yasuhito, Takahashi; Koji, Fujiwara

AIP ADVANCES **8**, 047501 (2018)

Simulation of the stress dependence of hysteresis loss using an energy-based domain model

Shumpei Ito,[1] Takeshi Mifune,[1] Tetsuji Matsuo,[1,a] Chikara Kaido,[2] Yasuhito Takahashi,[3] and Koji Fujiwara[3]
[1]*Kyoto University, Kyotodaigaku-katsura, Nishikyo-ku, Kyoto 615-8510, Japan*
[2]*Kitakushu National College of Technology, Kitakushu 802-0985, Japan*
[3]*Doshisha University, 1-3, Tatara Miyakodani, Kyotanabe, Kyoto 610-0321, Japan*

(Received 30 June 2017; accepted 23 August 2017; published online 16 October 2017)

The assembled domain structure model (ADSM) is a multiscale magnetization model that can be used to simulate the magnetic properties of a core material. This paper reveals the mechanism of the hysteresis loss increase due to compressive stress applied to a silicon steel sheet by conducting a simulation using the ADSM. A simple method of adjusting the simulated hysteresis loss to the measured loss is also proposed. By adjusting the hysteresis loss under a stress-free condition, the stress dependence of the hysteresis loss of a non-oriented silicon steel sheet is quantitatively reconstructed using the ADSM, where the stress-induced anisotropy strengthens the pinning effect along the stress direction. https://doi.org/10.1063/1.4993661

I. INTRODUCTION

The magneto-mechanical interaction in iron-core materials has been studied intensively to take into account magnetic deterioration due to compressive stressing of the motor core.[5–7] In representing the magneto-mechanical interaction, phenomenological modeling of the magnetization process is not useful because it requires parameter fitting of the measured property, yet a magnetic measurement under an arbitrary vector/tensor combination of magnetization and stress directions is practically difficult. Accordingly, a physical magnetization model is required to predict the stress dependence of hysteresis loss without a magnetic measurement under mechanical stress and the following model parameter fitting.

Several physical multiscale models[2,3,8] have successfully been used to predict the permeability decrease dependent on mechanical stress. However, the prediction of the stress dependence of the hysteresis-loss property[1,2,11] remains a challenging task because the physical modeling of the pinning field is an open problem.

The assembled domain structure model (ADSM)[3,4] is a physical magnetization model that includes the pinning effect on the crystal-grain scale. The model parameters are given by material constants, such as the anisotropy constant and magnetostriction constants. The magneto-elastic energy causes magneto-mechanical interaction in the core material, yielding stress-dependent magnetic properties.[3] The pinning field is simulated under an assumption of a statistical distribution of pinning sites.[3]

The main purpose of this paper is to reveal the mechanism of the loss increase due to the compressive stressing of a silicon steel sheet on the basis of simulation results obtained using the ADSM. A simple method of adjusting the simulated hysteresis loss using the ADSM to the measured loss is also proposed.

[a]Electronic mail: matsuo.tetsuji.5u@skyoto-u.ac.jp.

II. ADSM WITH A PINNING FIELD

The ADSM[3] (II.A) and pinning model[4] (II.B and C) are briefly explained.

A. ADSM

The ADSM is a multiscale model for which macroscopic magnetization is constructed by assembling mesoscopic cells called simplified domain structure models (SDSMs) (Fig. 1). An SDSM has six domains corresponding to the three easy axes of cubic anisotropy. The magnetization state in each cell is represented by the volume ratios r_i and the magnetization vectors $\boldsymbol{m}_i = (\sin\theta_i\cos\phi_i, \sin\theta_i\sin\phi_i, \cos\theta_i)$ $(i = 1 \ldots 6)$ of the six domains. The variable vector in a cell j is denoted $\boldsymbol{x}_j = (\theta_1, \ldots, \theta_6, \phi_1, \ldots, \phi_6, r_1, \ldots, r_5)$ $(r_6 = 1 - r_1 \ldots - r_5)$. The variable vectors $\boldsymbol{x}_j$ $(j = 1, 2, \ldots)$ are determined so as to give a local minimum of the total magnetic energy e, which consists of the Zeeman energy, crystalline anisotropy energy, magnetostatic energy, and magnetoelastic energy. For convenience of formulation, the energy components are normalized by the crystalline anisotropy constant while the magnetic field is normalized by the anisotropy field. For example, the normalized magnetoelastic energy is given as

$$e_{\mathrm{el}} = \sum_{i=1}^{6} r_i e_{\mathrm{el},i}, \tag{1}$$

$$e_{\mathrm{el},i} = -\frac{3\lambda_{100}}{2K}\sigma(\alpha_{1,i}^2\gamma_1^2 + \alpha_{2,i}^2\gamma_2^2 + \alpha_{3,i}^2\gamma_3^2) - 3\frac{\lambda_{111}}{K}\sigma(\alpha_{2,i}\alpha_{3,i}\gamma_2\gamma_3 + \alpha_{3,i}\alpha_{1,i}\gamma_3\gamma_1 + \alpha_{1,i}\alpha_{2,i}\gamma_1\gamma_2), \tag{2}$$

where σ is the stress, λ_{100} and λ_{111} are the magnetostriction constants, K is the crystalline anisotropy constant, $(\alpha_{1,i}, \alpha_{2,i}, \alpha_{3,i})$ and $(\gamma_1, \gamma_2, \gamma_3)$ are the direction cosines of the magnetization vectors of domain i and the stress σ with respect to the three easy axes of cubic anisotropy.

B. Distribution of the pinning field

Suppose that the macroscopic relationship between the normalized average magnetization m and the applied field h is represented as

$$h = h_{\mathrm{ah}}(m) + h_{\mathrm{p}}(m), \tag{3}$$

where $h_{\mathrm{ah}}(m)$ represents the anhysteretic magnetization curve and $h_{\mathrm{p}}(m)$ is the pinning field. The anhysteretic field is determined by Zeeman energy, crystalline anisotropic energy, magnetostatic energy, and magnetoelastic energy. The pinning field is additionally required to move a domain wall against friction generated by the pinning sites. The distribution of pinning sites is defined by a density function $f(p)$ satisfying

$$\int_0^\infty f(p)\mathrm{d}p = 1, \tag{4}$$

where p is the pinning strength.

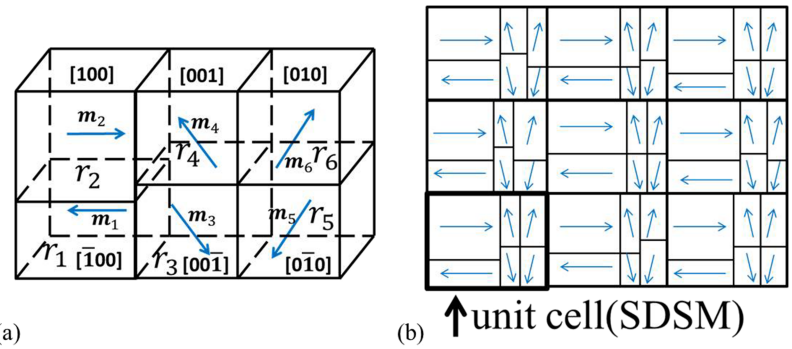

FIG. 1. Schematics of assembled domain structure model: (a) unit cell (SDSM) and (b) ADSM.

The magnetization proceeds with domain wall motions passing through pinning sites. In the case that the magnetization proceeds from the demagnetized state, the domain wall moves when $h_p = h - h_{ah}$ exceeds p and accordingly the magnetization is described as

$$m = \int_0^{hp} f(p)\mathrm{d}p, \tag{5}$$

The density function $f(p)$ is determined from the density of impurities or defects in the grains. This paper simply uses a Gaussian distribution as the density function. For convenience of simulation, relation (3) between h_p and m is reformulated using the scalar stop model[9] having input m and output $h_p(m) = h - h_{ah} = S(m)$, where $S(m)$ is a hysteretic function described by the stop model. The stop model is identified from the MH loops generated by the pinning model above.

C. Application to the ADSM

In the ADSM, the pinning field is added cell by cell. The pinning field h_p is additionally required to change the volume ratio r_i in a cell corresponding to the domain wall motion. The energy minimization procedure requires terms of $-\partial e/\partial r_i$ to decrease the total energy by changing r_i. To consider the pinning effect, the pinning energy e_p in every cell is added to e, where $\partial e_p/\partial r_i$ is the pinning field h_p in the cell. Accordingly, the effective field $-\partial e_p/\partial r_i$ refers to the force of friction acting on the domain wall.

For simplicity, suppose that the magnetization proceeds with 180° domain wall motion with two domains i and i' in a cell. The normalized magnetization along direction i in the cell is then given by $m_{cell} = 2r_i - 1$. Accordingly, the pinning field generated by the domain wall motion i is given as $h_p(m_{cell}) = h_p(2r_i - 1)$. Thus, $\partial e_p/\partial r_i$ is expressed as

$$\partial e_p/\partial r_i = 2h_p(2r_i - 1) = S(2r_i - 1). \tag{6}$$

Terms $\partial e_p/\partial \phi_i$ and $\partial e_p/\partial \theta_i$ are set to zero.

D. Adjustment of hysteresis loss

This paper proposes a method for adjusting the simulated hysteresis loss to the measured loss using a weighting function of the stop model.[10] The stop model with weighting function is given as

$$S_W(m) = w(m)S(m) \tag{7}$$

where $w(m)$ is the weighting function. Ref. 10 introduced an iterative method to determine the weighting function as

$$w^{k+1}(m) = \frac{L_{measured}(m)}{L_{simulated}(m)} w^k(m), \quad w^0(m) = 1 \tag{8}$$

where k is the iteration number, $L_{simulated}$ is the hysteresis loss for amplitude m computed using the ADSM with $w^k(m)S(m)$ and $L_{measured}$ is the measured loss. For simplicity, this paper sets $w(m) = w^1(m)$, which means that the adjustment of loss is not very accurate. Using $w(m)$, the pinning field is described as

$$\partial e_p/\partial r_i = S_W(2r_i - 1) = w(2r_i - 1)S(2r_i - 1). \tag{9}$$

This adjustment is a kind of parameter fitting using loss measurements. This paper aims to predict the hysteresis loss under mechanical stress from the hysteresis loss without stress. Hence, the weighting function is determined from the measured hysteresis loss without stress.

III. RESULTS AND DISCUSSIONS

A. Stress-dependent magnetic property

The magnetization process of a NO silicon steel sheet is simulated using $8 \times 8 \times 1$ cells where the unit cell dimension ratio is $1{:}1{:}10^{-4}$. The material constants used are the anisotropy constant for cubic anisotropy $K = 3.8 \times 10^4$ J/m^3, $\lambda_{100} = 2.3 \times 10^{-5}$, $\lambda_{111} = -1.0 \times 10^{-5}$ and $\mu_0 M_S = 2.2$ T. The crystal orientations in the 64 cells are randomly distributed. The density function $f(p)$ is given by a Gaussian distribution whose average and variance are 9.2×10^{-4} and 6.2×10^{-8}, respectively.

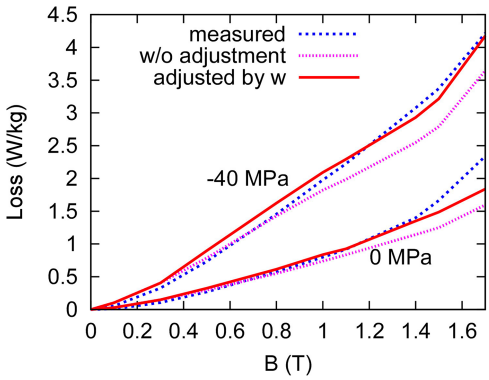

FIG. 2. Simulated and measured hysteresis losses along the RD with and without mechanical stress.

Figure 2 shows the simulated hysteresis loss at 50 Hz with and without mechanical stress along the rolling direction (RD). The weighting function improves the representation of hysteresis loss over 1 T under a stress-free condition. A quantitative agreement of the loss increase due to compressive stress is obtained. Figure 3 shows BH loops with and without stress, where the simulated loops roughly agree with measured loops and the decrease in permeability due to compressive stress is predicted using the ADSM.

B. Dependence of hysteresis loss on mechanical loss

Figure 4 shows the dependence of hysteresis loss on the applied stress along the RD. The weighting function improves the loss property representation at 1.5 T. If the simulated hysteresis loss without stress agrees with the measured loss, the loss increase due to compressive stress is accurately represented. The tensile stress does not affect the loss appreciably.

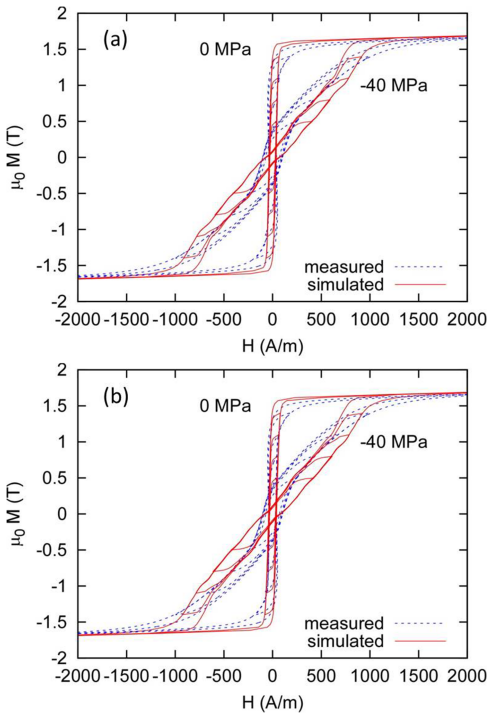

FIG. 3. Measured and simulated MH loops along the RD under stress-free condition and compressive stress of 40 MPa when amplitude is $\mu_0 M$ = 0.5, 0.8, 1.1, 1.4, 1.7 T: (a) without and (b) with a weighting function.

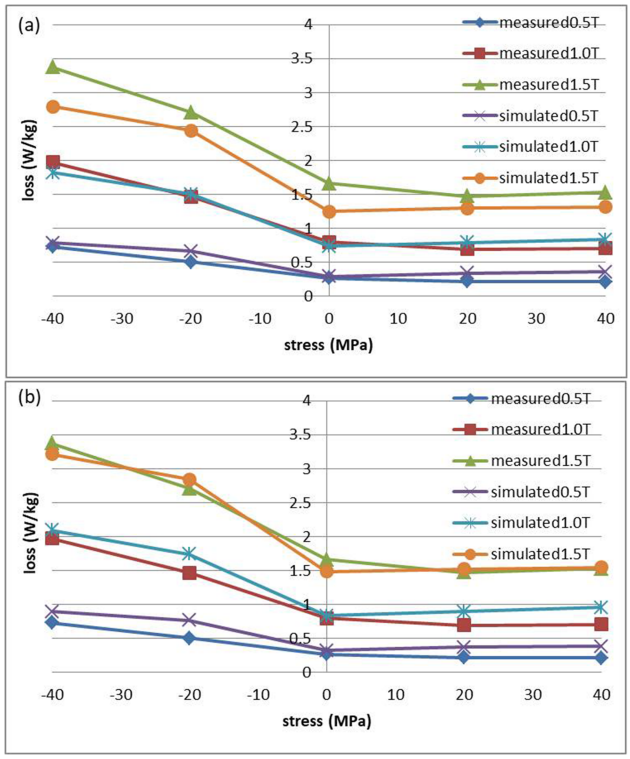

FIG. 4. Dependence of hysteresis loss on applied stress when amplitude of $\mu_0 M$ is 0.5, 1.0, 1.5 T: (a) without and (b) with a weighting function.

Supposing that the magnetization vector of domain i is directed along one of the easy axes ($\alpha_{1,\,i} = 1$, $\alpha_{2,\,i} = \alpha_{3,\,i} = 0$), Eq. (2) gives

$$e_{\mathrm{el},i} = -\frac{3\lambda_{100}}{2K}\sigma\gamma_1^2. \tag{10}$$

Equation (9) has unidirectional anisotropy, where the stress direction of compressive or tensile stress becomes the hard or easy axis of magnetization, respectively. Figure 5 shows the distribution of magnetization directions in the domains of 8×8 cells with/without stress, where the distribution of the angle difference $|\beta|$ between the magnetization direction and the RD is shown.

At the demagnetizing state ($m = 0$), the distribution of $|\beta|$ is almost symmetric with respect to $|\beta| = \pi/2$ to cancel the average magnetization by pairs of domains having anti-parallel magnetization

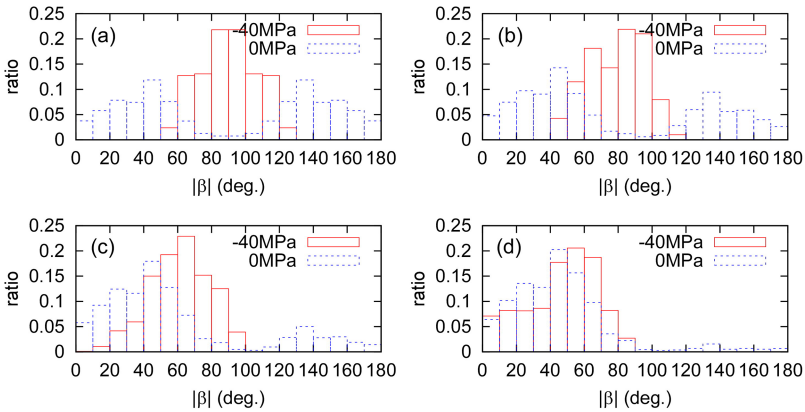

FIG. 5. Distribution of the magnetization angle $|\beta|$ from the RD: (a) when $\mu_0 M = 0$ T, (b) 0.4 T, (c) 1.0 T, and (d) 1.4 T.

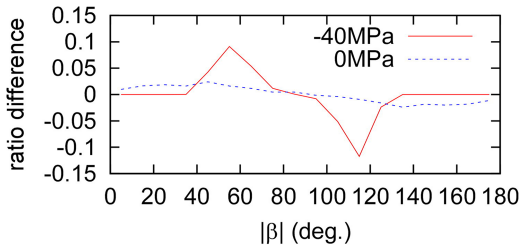

FIG. 6. Difference of magnetization angle between $\mu_0 M = 0$ and 0.4 T.

vectors with $|\beta|$ and $\pi - |\beta|$. The magnetization direction is randomly distributed at the demagnetizing state ($m = 0$) under the stress-free condition. Under the stress-free condition, the magnetization dominantly proceeds with 180° domain wall motion, which is shown by the shift of the distribution from the angle $|\beta|$ to $\pi - |\beta|$.

When compressive stress is applied along the RD, the magnetization is nearly perpendicular to the RD in the demagnetizing state because of the stress-induced anisotropy. Under compressive stress, the magnetization also proceeds with 180° domain wall motion roughly within $60° \leq |\beta| \leq 120°$ when the magnetization is small. Figure 6 plots the difference of $|\beta|$ between $\mu_0 M = 0$ and 0.4 T, where the distribution is almost point-symmetric with respect to $(\pi/2, 0)$ showing the shift of the distribution from $|\beta|$ to $\pi - |\beta|$. When the magnetization becomes large, there is a shift of the distribution from $|\beta|$ to nearly $|\beta| - \pi/2$, which corresponds to the 90° domain wall motion. The compressive stress thus increases the 180° domain wall motion roughly within $\pi/3 \leq |\beta| \leq 2\pi/3$ and the 90° domain wall motion, which strengthens the pinning field as follows.

If the magnetization proceeds with 180° domain wall motion between two domains, the magnetization along the RD is

$$m_{\text{cell}} = (2r - 1)\cos\beta, \tag{11}$$

where the volume ratio of the two domains are r and $1 - r$ having the magnetization angles of β and $\beta + \pi$. The domain motion $\Delta r = \Delta m_{\text{cell}}/(2\cos\beta)$ increases if β is near $\pi/2$, which results in a strong pinning field. If the magnetization proceeds with 90° domain wall motion between two domains having magnetization angles of β and $\beta \pm \pi/2$, for example, the magnetization along the RD is

$$m_{\text{cell}} = r\cos\beta + (1 - r)\cos(\beta \pm \pi/2) = r\cos\beta \pm (r - 1)\sin\beta. \tag{12}$$

The domain motion $\Delta r = \Delta m_{\text{cell}}/(\cos\beta \pm \sin\beta)$ exceeds 180° domain wall motion with $\beta \approx 0$. The ADSM can predict the loss increase due to the compressive stress because it describes the effect of stress on the magnetization state in the crystal-grain scale depending on the distributed crystal orientations.

IV. CONCLUSION

The mechanism of hysteresis loss increase due to compressive stress was discussed according to simulation results obtained using the ADSM. The dependence of hysteresis loss on the applied stress was predicted using the ADSM, and agrees with the measured loss property quantitatively. The simulated distribution of magnetization angles shows that the compressive stress suppresses the development of magnetic domains having magnetization nearly parallel/antiparallel to the stress direction. As a result, the compressive stress causes mechanically induced anisotropy that increases the hysteresis loss by strengthening the pinning field along the compressed direction in the process of domain wall motion.

ACKNOWLEDGMENTS

This work was supported in part by the Japan Society for the Promotion of Science under Grant-in-Aid for Scientific Research (C) Grant No. 26420232.

[1] L. Daniel, M. Rekik, and O. Hubert, "A multiscale model for magneto-elastic behaviour including hysteresis effects," Arch. Appl. Mech. **84**, 1307–1323 (2014).
[2] Fujisaki, J., Furuya, A., Uehara, Y., Shimizu, K., Oshima, H., Sasayama, T., and Takahashi, N., "Hysteresis Modeling of a Non-Oriented Electrical Steel Sheet under Compressive Stress," Proc. Joint Tech. Meeting Static App. Rotating Mach., SA-13–72/RM-13-86 (2013).
[3] S. Ito, T. Mifune, T. Matsuo, and C. Kaido, "Macroscopic magnetization modeling of silicon steel sheets using an assembly of six-domain particles," J. Appl. Phys. **117**, 17D126 (2015).
[4] Ito, S., Mifune, T., Matsuo, T., Kaido, C., Takahashi, Y., and Fujiwara, K., "Domain structure model including pinning effect based on the statistical distribution function," IEEJ Trans. F.A. submitted.
[5] Y. Kai, Y. Tsuchida, T. Todaka, and M. Enokizono, "Influence of stress on vector magnetic property under alternating magnetic flux conditions," IEEE Trans. Magn. **47**, 4344–4347 (2011).
[6] C. Kaido, N. Hirose, S. Iwasa, T. Hayashi, and Y. Waki, "Stress dependence of magnetic properties in non-oriented electrical steel sheets," J. Magn. Soc. Jpn. **34**, 140–145 (2010).
[7] M. LoBue, C. Sasso, V. Basso, F. Fiorillo, and G. Bertotti, "Power losses and magnetization process in Fe Si non-oriented steels under tensile and compressive stress," J. Magn. Magn. Mater. **215–216**, 124–126 (2000).
[8] O. Hubert and L. Daniel, "Multiscale modeling of the magneto-mechanical behavior of grain-oriented silicon steels," J. Magn. Magn. Mater. **320**, 1412–1422 (2008).
[9] T. Matsuo and M. Shimasaki, "Isotropic vector hysteresis represented by superposition of stop hysteron models," IEEE Trans. Magn. **37**, 3357–3361 (2001).
[10] T. Matsuo, "Comparison of rotational hysteretic properties of isotropic vector stop models," IEEE Trans. Magn. **45**, 1194–1197 (2009).
[11] D. Singh, F. Martin, P. Rasilo, and A. Belachen, "Magnetomechanical model for hysteresis in electrical steel sheet," IEEE Trans. Magn **52**, 7301109 (2016).